AD-A286 524

IENTATION PAGE Dist: A

timated to average 1 hour per response, including the time for reviewing instructions, searching existing data sources, and reviewing the collection of information. Send comments regarding this burden estimate or any other aspect of this burden, to Washington Headquarters Services, Directorate for Information Operations and Reports, 1215 Jefferson the Office of Management and Budget, Paperwork Reduction Project (0704-0188), Washington, DC 20503.

1. AGENCY USE ONLY (Leave blank)	2. REPORT DATE August 1994	3. REPORT TYPE AND DATES COVERED Reprint

4. TITLE AND SUBTITLE Laser-induced thermal acoustics (LITA): (U) four-wave mixing measurement of sound speed, thermal diffusivity, and viscosity	5. FUNDING NUMBERS PE - 61103D PR - 3484 SA - AS

6. AUTHOR(S) Eric B. Cummings	G - F49620-93-1-0338

7. PERFORMING ORGANIZATION NAME(S) AND ADDRESS(ES) Calfiornia Institute of Technology 1201 E. California Blvd Pasadena, CA 91125	8. PERFORMING ORGANIZATION REPORT NUMBER AFOSR-TR· 94 0738

DTIC ELECTE NOV 28 1994 B

9. SPONSORING/MONITORING AGENCY NAME(S) AND ADDRESS(ES) AFOSR/NA 110 Duncan Avenue, Suite B115 Bolling AFB DC 20332-0001	10. SPONSORING/MONITORING AGENCY REPORT NUMBER

12a. DISTRIBUTION/AVAILABILITY STATEMENT Approved for public release; distribution is unlimited	12b. DISTRIBUTION CODE A

13. ABSTRACT (Maximum 200 words)

Laser-induced thermal acoustics (LITA) is a promising optical four-wave mixing technique for gasdynamic measurement. The $\chi^{(3)}$ nonlinear process is a sequence of two opto-acoustic effects, electrostriction and absorption/rapid thermalization, and the acousto-optic effect. The evolution of the laser-induced acoustic structures temporally modulates $\chi^{(3)}$ and thereby the LITA signal. Time resolution of the signal provides the sound speed, thermal diffusivity, and acoustic damping rate, along with information about atomic or molecular energy transfer rates. LITA can also measure spectra of both the real and imaginary gas susceptibility. The physics of LITA is discussed and the derivation is sketched of a simple analytical expression that accurately describes both the magnitude and time history of the LITA signal. Early experimental results are presented. Sound speeds accurate to 0.5% and transport properties accurate to 30% have been measured in a single-shot without calibration. More realistic modeling should dramatically improve transport-property measurement. LITA "spectra" have been taken of weak spectral lines of NO, in concentrations less than 50 ppb. Signal reflectivities as high as 10^{-4} have been estimated. New applications of LITA, including velocimetry, are suggested.

20060713012

BEST AVAILABLE COPY

14. SUBJECT TERMS LITA, four-wave mixing, thermal acoustics, single-shot measurement, velocimetry	15. NUMBER OF PAGES 10
	16. PRICE CODE

17. SECURITY CLASSIFICATION OF REPORT Unclassified	18. SECURITY CLASSIFICATION OF THIS PAGE Unclassified	19. SECURITY CLASSIFICATION OF ABSTRACT Unclassified	20. LIMITATION OF ABSTRACT UL

Standard Form 298 (Rev. 2-89)
Prescribed by ANSI Std. 239-18
298-102

LASER-INDUCED THERMAL ACOUSTICS (LITA)
FOUR-WAVE MIXING MEASUREMENT OF SOUND SPEED, THERMAL DIFFUSIVITY, AND VISCOSITY

E.B. Cummings
GRADUATE AERONAUTICAL LABORATORIES
CALIFORNIA INSTITUTE OF TECHNOLOGY
Pasadena, CA 91125

Laser-induced thermal acoustics (LITA) is a promising optical four-wave mixing technique for gasdynamic measurement. The $\chi^{(3)}$ nonlinear process is a sequence of two opto-acoustic effects, electrostriction and absorption/rapid-thermalization, and the acousto-optic effect. The evolution of the laser-induced acoustic structures temporally modulates $\chi^{(3)}$ and thereby the LITA signal. Time resolution of the signal provides the sound speed, thermal diffusivity, and acoustic damping rate, along with information about atomic or molecular energy transfer rates. LITA can also measure spectra of both the real and imaginary gas susceptibility. The physics of LITA is discussed and the derivation is sketched of a simple analytical expression that accurately describes both the magnitude and time history of the LITA signal. Early experimental results are presented. Sound speeds accurate to 0.5% and transport properties accurate to 30% have been measured in a single shot without calibration. More realistic modeling should dramatically improve transport property measurement. LITA "spectra" have been taken of weak spectral lines of NO_2 in concentrations less than 50 ppb. Signal reflectivities as high as 10^{-4} have been estimated. New applications of LITA, including velocimetry, are suggested.

Introduction

A new optical diagnostic technique for single-shot point measurement of gasdynamic parameters has been developed at GALCIT. This technique, named Laser Induced Thermal Acoustics (LITA), uses the time-resolved signal generated via four-wave mixing to measure the sound speed, thermal diffusivity and acoustic damping coefficient (and thereby viscosity) of a gas. If a gas behaves according to a known caloric equation of state, the temperature of the gas may be inferred from the sound speed. This technique is similar to the LIPS (laser induced phonon scattering) technique for the measurement of sound speeds in crystals[1,2]. Using completely uncalibrated single-shot LITA, the temperature of the laboratory air was measured within 0.5%, limited by uncertainty of the molecular weight of the humid air and beam geometry. The thermal diffusivity and acoustic damping coefficient were measured within 30% of published values, limited by finite beam size and thermalization-rate effects, which were ignored. "Calibration" to improve the accuracy of the transport property measurement involves the determination of thermalization rates, and the measurement of beam profiles.

The geometry of the LITA experiment is similar to that of CARS (coherent anti-Stokes Raman scattering) or DFWM (degenerate four wave mixing). However the nonlinearity producing the LITA signal is a combination of opto-acoustic and acousto-optic effects, not the coherent superposition of quantum mechanical states used in the other techniques. An analytical expression for the absolute amplitude and time history of the LITA signal has been derived assuming linear hydrodynamic gas behavior[3]. This analysis has shown that LITA signals may rival LIF (laser induced fluorescence) or DFWM signals in intensity when comparable lasers are used.

To date, two opto-acoustic phenomena have produced LITA signals. The first is electrostriction, in which molecules of a polarizable gas minimize their potential energy by clustering in regions of high optical electric field intensity[4]. When the optical field is removed, the clustered gas molecules are released emitting sound waves in the manner of a popped balloon. Electrostriction produces a LITA signal proportional to the square of the real part of the gas susceptibility that may be nonresonant or resonantly enhanced. The second opto-acoustic phenomenon is absorption followed by rapid nonradiative decay or "thermalization" of absorbed energy. Rapid thermalization causes rapid expansion of the gas, inducing sound waves. The LITA signal from this effect is proportional to the square of the imaginary part of the gas susceptibility. The two phenomena produce LITA signals with different signatures allowing sorting of the contribution to the LITA signal from each effect. Thus, a spectrum of both the real and imaginary parts of the gas susceptibility may be measured using LITA. This principle was demonstrated using weak transitions near the sodium D lines of the laboratory air trace species NO_2 less than 50 ppb.

LITA spectra occur on hydrodynamic time scales and depend upon bulk or continuum properties of a highly collisional gas. This makes LITA unique among laser diagnostics, most of which occur on molecular time scales and deduce molecular-molecular interactions. LITA benefits from strong excited-state energy quenching, a molecular interaction that hampers LIF and other spectroscopic techniques. LITA measurements have a unusual advantage where molecular densities and quenching rates

are high, as in many flows of practical gas-dynamic and aerothermochemical interest. For example, high molecular density is a requirement for the rapid chemical reactions needed in advanced propulsion systems. The hydrodynamic lifetime of the LITA interaction suggests new applications of the technique, among which are measurement of velocity by analogy with laser Doppler velocimetry and measurement of vorticity, for which there is no conventional analog.

This article outlines the development and early experiments of this measurement technique. First, the physics of LITA measurements is discussed. A brief sketch follows of the derivation of the analytical expression for the LITA signal. The experimental setup used at GALCIT is then presented along with the results of the early experiments. Finally, future directions are suggested for LITA application and conclusions are drawn.

Physics of LITA

LITA is a laser-induced dynamic grating technique similar to CARS and DFWM. The principal difference between these techniques and LITA is the $\chi^{(3)}$ (nonlinear) process that produces the signal. LITA employs a combination of opto-acoustic and acousto-optic effects. Light from a powerful, fast-pulsed "driver" laser (e.g., 1 - 1000 mJ, 1 - 10 ns) generates acoustic waves by two opto-acoustic effects, electrostriction and rapid thermalization.

The former effect is caused by the tendency of polarizable molecules to minimize their potential energy by clustering in regions of high optical electric field intensity[1]. Electrostriction has the effect of lowering the pressure in regions of high field. When the field is removed, there is a pressure unbalance that propagates as acoustic waves. This effect is proportional to the real part of the gas susceptibility.

The latter effect is a multiple step process that relies upon molecular collisions. First, molecules of the gas absorb energy from the driver laser and store it in excited states when the driver laser resonates with an absorption line of the gas. Next, inelastic molecular collisions convert part of the excited-state energy to molecular kinetic or rotational energy. This conversion may require only a few collisions (e.g. 5-10) or many (e.g., hundreds), depending upon the composition of the gas. Finally, elastic molecular collisions equilibrate the velocities of the molecules resulting in a rise in temperature. This equilibration usually requires only a few collisions (e.g. five to ten). The term "thermalization" covers the conversion of laser energy to thermal energy. Thermalization is proportional to the imaginary part of the gas susceptibility.

In order for the thermalization to produce acoustic waves efficiently, the drop in gas density accompanying the rise in temperature must sharply lag that of equilibration. The density should be "frozen" on the time scale of thermalization (τ_{th}). Density changes in a medium travel characteristically at the sound speed (c_s). Thermalization must occur on a time scale comparable to or less than the time for density changes to travel across a characteristic LITA length scale (Λ_g), the length scale over which the intensity of the driver laser varies

$$\tau_{th} \cdot \frac{\Lambda_g}{c_s} \tag{1}$$

Because τ_{th} is inversely proportional to the collision rate, this effect becomes more efficient as density increases. At atmospheric densities and temperatures, LITA data showed that fast thermalization times were of the order five to fifteen nanoseconds for the NO_2 excited states used in these experiments (of the order ten collisions[6]). This compares with Λ_g/c_s of thirty to one-hundred nanoseconds. The acoustic fields generated by the driver laser evolve in time and space. They are damped by thermal diffusivity and viscosity. Under the conditions studied in these experiments, this damping occurs on the microsecond time scale.

Light from a long-pulse or CW "source" laser scatters into the LITA signal by an acousto-optic effect. Because the susceptibility of a medium is nearly linear with density for acoustic disturbances[1], the density perturbation field of the acoustic waves generates a corresponding susceptibility perturbation field. The susceptibility field scatters light from the source laser, forming the LITA signal. Analysis of the time-history of the scattered signal provides information about the speed and decay of the opto-acoustic disturbances and thereby the sound speed and transport properties of the gas

Adopting a four-wave mixing geometry for LITA as shown in Figure 1 provides both spatial resolution and coherent signal enhancement. The driver laser is split into two beams which cross at a small angle (0.5 - 5 degrees) in the gas. The LITA signal is generated only in the sample volume, where these beams intersect, providing spatial resolution. Because the driver beams are coherent with each other, they interfere with each other in the form of an ellipsoidal grating at their intersection. The grating wavelength Λ_g is given by

$$\Lambda_g \cdot \frac{\lambda_d}{2\sin\frac{\theta}{2}} \tag{2}$$

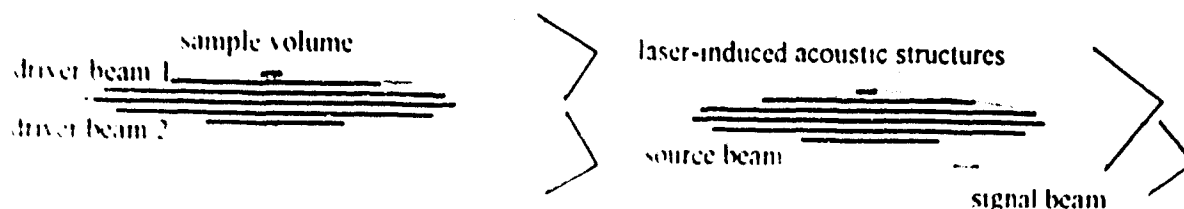where λ_d is the driver laser wavelength and θ is the beam-crossing angle

Figure 1   A forward-scattering LITA geometry was used in these experiments. The driver beams write acoustic gratings into the gas. The source beam incident at the Bragg angle scatters off the acoustic structures into a coherent signal beam.

The opto-acoustic effects generate acoustic structures (modulation depth 0.01 – 5%) initially in the shape of the ellipsoidal grating. The nature of the acoustic structures generated by the two effects is different. Electrostriction forms two traveling acoustic wavepackets (phonons) and a very weak stationary isobaric density grating (thermon) each with the wavelength of the electric field grating. Thermalization generates the same acoustic structures but the "thermon" is dominant. The phonons counterpropagate in the direction parallel to the grating vector and decay by acoustic damping. The thermon decays by heat conduction. Light scattered from the source laser by the acoustic grating structures adds coherently when the source laser is incident at the Bragg angle of the grating. As shown in Figure 1, the Bragg-scattered light emerges in a lobe or laser-like beam, which may be efficiently detected with large f-number optics. This feature is attractive where optical access is limited or where luminosity mandates large f-number detection.

Each acoustic structure scatters light from the source laser onto the detector. If there is no convection velocity, light scattered by the phonon moving upward in Figure 1 has a Doppler "red-shift." Light scattered by its conjugate phonon has a Doppler "blue-shift." Light scattered by the thermon has no Doppler shift. The beating between the light scattered by these structures modulates the signal seen by the square-law detector. Three frequency components are present in the signal modulation (neglecting damping): a DC component, a component at the "Brillouin" frequency, c_s / Λ_g, caused by phonon/thermon signal mixing, and a component at twice the Brillouin frequency, caused by mixing of signals generated by the conjugate phonons. A strong phonon/thermon frequency component is only present if the thermalization effect is present. This additional frequency component allows distinction of the thermalization and electrostriction effects when the two are of comparable magnitude. The real and imaginary parts of the gas susceptibility may thus be measured independently using LITA.

Analysis of LITA Signals

This section outlines the derivation of an analytical expression for the amplitude and time history of the LITA signal. This expression allows the magnitude of LITA signals to be estimated *a priori* for experimental feasibility studies and the actual LITA signal to be interpreted quantitatively, with very good experimental agreement. The analysis treats the opto-acoustic effects and the hydrodynamic evolution of the acoustic structures using the linearized hydrodynamic equations[ ]. The perturbation solution for the far field of light scattered off a dielectric disturbance accounts for the acousto-optical effect[ ]. A simple analytical result is obtained for short-duration Gaussian driver beams, infinite-extent, monochromatic source beam, and single-rate-dominated thermalization[3].

Opto-acoustic effects appear as source terms in the closed set of linearized hydrodynamic continuity, momentum, and energy equations. Thermalization behaves like a temperature source in the energy equation while electrostriction forces the momentum equation. In terms of perturbations in density (ρ), temperature, (T), these equations are

$$\frac{\partial \rho_1}{\partial t} + \rho c_1 = 0, \tag{3}$$

$$\frac{\partial c_1}{\partial t} + \frac{c_s^2 \nabla^2 \rho_1}{\gamma \rho} + \frac{\alpha c_s^2}{\gamma} \nabla^2 T_1 - D_l \nabla^2 c_1 = c_s, \tag{4}$$

$$\frac{\partial T_1}{\partial t} - \frac{\gamma - 1}{\alpha \rho} \frac{\partial \rho_1}{\partial t} - \gamma D_T \nabla^2 T_1 = T_{th}. \tag{5}$$

where perturbation terms are indicated by the subscript '1', $\psi_1 \equiv \nabla \cdot u_1$, and $\nabla^2 \equiv \partial^2/\partial x^2 + \partial^2/\partial y^2 + \partial^2/\partial z^2$. The parameter γ is the ratio of specific heats of the medium (c_p/c_v), α is the thermal expansion coefficient ($-(1/\rho)(\partial\rho/\partial T)_p$), c_s is the isentropic sound speed, D_V is the longitudinal kinematic viscosity ($1/\rho(\eta_v + (4/3)\eta_s)$), and D_T is the thermal diffusivity. The boundary and initial conditions are

$$\rho_1(\mathbf{r}, t=0) = 0; \qquad \psi_1(\mathbf{r}, t=0) = 0; \qquad T_1(\mathbf{r}, t=0) = 0, \tag{6}$$

$$\rho_1(\mathbf{r}, t) \to 0; \qquad \psi_1(\mathbf{r}, t) \to 0; \qquad T_1(\mathbf{r}, t) \to 0, \quad \text{as} \quad |\mathbf{r}| \to \infty.$$

Here, the mean flow velocity is assumed to be zero. This assumption leads to a loss of generality because of the lack of Galilean invariance of the system. The general case of arbitrary mean flow velocity will be explored in an upcoming extension of this work.

The electrostriction source term ($\dot{\psi}_\epsilon(\mathbf{r}, t)$) is approximately

$$\dot{\psi}_e \simeq \frac{\mathrm{Re}\{\chi(\omega_d)\}}{\rho} E_d \nabla^2 I(\mathbf{r})P(t), \tag{7}$$

for small density perturbations. The parameter E_d is the total energy of the driver beams during a pulse, $P(t)$ is the normalized temporal profile of the driver laser, $I(\mathbf{r})$ is the normalized driver laser field intensity in the sample volume. This term is proportional to the real part of the gas susceptibility at the driver frequency, ω_d, where $\chi \equiv \epsilon/\epsilon_0 - 1$.

The thermalization term $\dot{T}_{th}(\mathbf{r}, t)$ describes the conversion of energy from the driver laser beams to heat. While this process may be arbitrarily complicated, a single-rate rate equation for the excited state energy ($U(\mathbf{r}, t)$) with diffusion effects approximates the character of the process:

$$\dot{T}_d(\mathbf{r}, t) = \frac{\gamma_{th}}{\rho_0 c_v} U(\mathbf{r}, t). \tag{8}$$

where

$$\frac{\partial U}{\partial t} + \gamma_{th}U + \gamma_{nth}U - D_e\nabla^2 U = -2\omega_d \mathrm{Im}\{\chi(\omega_d)\} E_d I(\mathbf{r})P(t). \tag{9}$$

$$U(\mathbf{r}, t=0) = 0.$$

where $U(\mathbf{r}, t)$ is the excited-state energy density field, γ_{th} is the rate of loss of excited-state energy to thermal energy, γ_{nth} is the rate of excited-state energy loss other than to thermal energy, D_e is the diffusivity through the gas of excited molecules, and c_v is the heat capacity of the gas at constant volume. If thermalization is rapid enough, $\dot{T}_{th}$ behaves like a delta function rendering the hydrodynamic behavior thermalization-rate insensitive. If a single thermalization rate model does not adequately describe the system, the linearity of the equations allows solutions using different rates to be superimposed to simulate a more complicated energy conversion. Thermalization was approximated by independent fast (e.g., 10 ns) and slow (e.g., 100 ns) processes to fit the LITA data presented later.

Equations 3, 4, 5, and 9 may be solved by applying Fourier and Laplace transforms[7,3]. The resulting set of linear algebraic equations has the solution in terms of the Fourier transform and Laplace variables q and s respectively:

$$\frac{\rho_1(\mathbf{q}, s)}{\rho} = \frac{E_d q^2 I(\mathbf{q})}{\rho} \frac{P(s)}{M(q, s)} \left[-(s + \gamma D_T q^2)\mathrm{Re}\{\chi(\omega_d)\} + \frac{2(\gamma - 1)\gamma_{th}\omega_d}{(s + \gamma_{th} + \gamma_{nth} + D_e q^2)} \mathrm{Im}\{\chi(\omega_d)\} \right], \tag{10}$$

where perfect gas behavior has been assumed. The quantity $M(q, s)$ is the characteristic equation of the system of algebraic equations.

$$M(q, s) = s^3 + (D_v q^2 + \gamma D_T q^2)s^2 + (c_s^2 q^2 + \gamma D_T q^2 D_v q^2)s + c_s^2 q^2 D_T q^2. \tag{11}$$

The roots of the cubic equation $M(s, q) = 0$, provided Λ_q is much larger than the mean-free path of the gas, are very nearly

$$s_1 = -D_T q^2.$$

$$s_2 = -\Gamma q^2 + ic_s q, \quad \text{and} \tag{12}$$

$$s_3 = -\Gamma q^2 - ic_s q.$$

where Γ is the classical acoustic damping coefficient, $(1/2[(\gamma - 1)D_T + D_V])$, and c_s is the isentropic speed of sound.

A partial fractions expansion of equation 10 in the roots of s simplifies Laplace inversion. There are four terms in this expansion. Two terms corresponding to the real roots of the denominator combine to describe the formation and decay of a thermon. The terms resulting from the two imaginary roots describe the formation of conjugate phonons. The acousto-optical effect is modeled using the perturbation solution[8] for the far-field of light, E_s, scattered from a source beam by a small disturbance in the susceptibility at the source-beam wavelength, $\chi_1(r, t; \omega_0)$.

$$E_s(\mathbf{R}, t; \mathbf{q}) = -\frac{E_0 k_s^2}{4\pi R} \exp i(\mathbf{k}_s \cdot \mathbf{r} - \omega_0 t)\chi_1(\mathbf{q}, t; \omega_0). \tag{13}$$

where q is the change in wave vector from the source to the scattered beam. The scattering direction and strength are dictated by the spatial Fourier transform of the susceptibility disturbance:

$$\chi_1(\mathbf{q}, t; \omega_0) = \int_{-\infty}^{\infty} d^3 r \exp(i\mathbf{q} \cdot \mathbf{r})\{\chi_1(\mathbf{r}, t; \omega_0)\}. \tag{14}$$

The susceptibility of a gas is closely proportional to the gas density for small density changes, thus,

$$\chi_1(\mathbf{q}, t; \omega_0) \simeq \chi(\omega_0)\frac{\rho_1(\mathbf{q}, t)}{\rho}. \tag{15}$$

The right-hand side of this equation is known in terms of the driver laser parameters. Thus, combining equations 10, 13, and 15, the scattered light field is known in terms of the imposed lasers and parameters of the gas medium including the sound speed, thermal diffusivity, and acoustic damping coefficient.

The scattered signal emerges as a coherent beam with the divergence angle limited by diffraction from the small sample volume. Integrating the square of the scattered electric field over the detector area yields the total LITA signal intensity. Signal strength may be expressed as a reflectivity, or ratio of the signal beam to source beam intensity. The magnitude of the LITA reflectivity is of the order 10^{-4} for room air with a thermal modulation depth of 1% in a two-millimeter-long sample volume, without resonant enhancement at the source-laser wavelength. Experiments at GALCIT used a one-Watt CW Ar Ion laser for the source laser. From reflectivities of this magnitude, a milliwatt-range He-Ne source laser could provide usable signal levels.

In the limit of rapid thermalization, short driver-laser duration, and flat source-beam intensity, the expression for the temporal LITA signal becomes

$$I_{LITA}(t) \propto (A\exp\{-D_t q_g^2 t\} + B\cos\{c_s q_g t + \Phi\}\exp\{-\Gamma q_g^2 t\})^2. \tag{16}$$

where $q_g \equiv 2\pi/\Lambda_g$ is the driver beam interference grating vector, and A, B, and Φ are simple algebraic functions of gas and laser beam parameters. Where the approximations listed above are not valid, spatial and temporal convolutions of laser-beam profiles augment the analysis. While generally these convolutions require numerics, all of the parameters which augment the analysis are readily measured except the thermalization rates. These rates may either be inferred from the LITA data, estimated from published data, or ignored provided they are much faster than the acoustic motion.

LITA Experimental Setup

The philosophy behind the development of LITA has been to obtain the most accurate and robust gas-dynamic measurements with the least experimental and analytical complexity. Common and relatively inexpensive tuneable or fixed-frequency lasers may be used for LITA. While LITA requires wide-handwidth signal detection and recording, and geometrical phase-matching, these experimental complications are offset by the intensity of the LITA signals and the ease in signal analysis. Furthermore, LITA measurement of the sound speed provides the gas temperature if the caloric equation of state of the gas is known. Other spectroscopic techniques usually measure temperature by scanning a rotational band of a well-studied diatomic molecule with accessible transitions, of which there is only a handful. The populations of these bands must be inferred from the signals, not a trivial practice in some diagnostics, and then fit to a Boltzmann distribution to obtain temperature. LITA thermometry may be done entirely nonresonantly or resonantly using any absorption line, provided some absorbed energy is thermalized on the LITA time-scale or faster. This freedom in absorption-line choice may significantly simplify experiments by eliminating the need for frequency conversions into the UV or IR.

Figure 2 shows a schematic diagram of the experimental apparatus used in LITA experiments at GALCIT. The driver laser is a home-brew narrowband pulsed dye laser oscillator/amplifier with a noise bandwidth of about 3 GHz. Pumped by a Continuum Q-switched, frequency-doubled Nd:YAG laser model YG-660 at about 150 mJ/pulse, the dye laser output is about 30 mJ in approximately 5 ns pulses. The laser operated from about 587 nm to about 592 nm during these experiments.
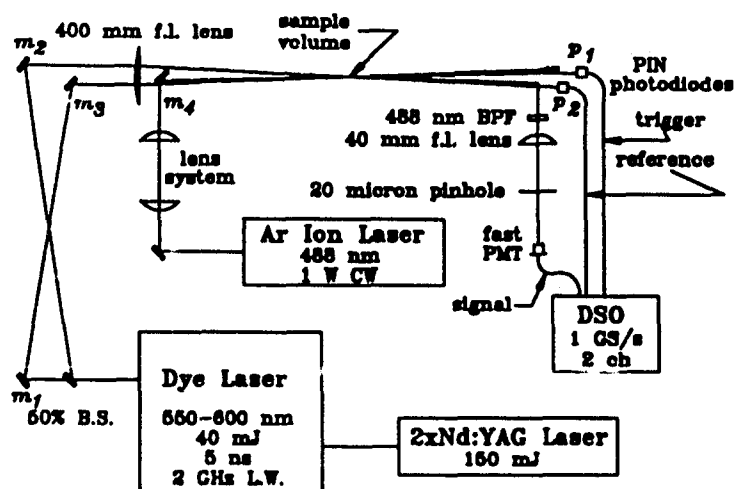

Figure 2.   The LITA experiments conducted at GALCIT use a Nd:YAG pumped dye-laser for the driver laser and a CW argon ion laser for the source. The LITA signal is detected by a fast PMT and recorded by a fast DSO.

Approximately three-millimeter-wide driver beams are formed from the dye laser emission by a 50% beam splitter and a mirror m_1. The crossing geometry of the beams ensures that both beams travel similar lengths to the sample volume so that phase coherence between the beams is not lost. Mirrors m_2 and m_3 are adjusted so that the driver beams are parallel and enter the 400 mm lens symmetrically. The driver beams intersect at the focus of the lens where they approximate finite plane waves about 200 μm in diameter. The beam crossing angle is set by the distance between the parallel beams, adjusted using micrometer translation stages under mirrors m_2 and m_3. BOXCARS geometries[5] with crossing angles ranging from $1.0°$ to $2.3°$ were used in these experiments. Detection of the driver beam pulse by a silicon PIN photodiode, p_1 (Thor labs, model DET-2SI), triggers the acquisition of the LITA signal. The source laser used in these experiments is a CW argon ion laser operating at 488 nm with a 1 W output power (Spectra Physics Model 165). The source laser should have a coherence length longer than the interaction region, typically two to ten millimeters, because phase noise of the source laser manifests itself in the washing-out of the modulation of the signal beam. Future experiments are planned using a flashlamp-pumped dye laser with a pulse duration of about 800 ns, a pulse energy up to 3 J, and a linewidth of about 0.003 nm. Under the same conditions, this laser will provide one million times the signal obtained from the Ar ion laser, providing incoherent-scattering-limited sensitivity.

The source beam passes through a two-lens system which adjusts the beam width, ranging from about 200 μm to 2 mm in these experiments. The mirror m_1 points the source beam at the sample volume. Phase-matching adjustments are made using a micrometer-driven translation stage under m_1. A silicon PIN photodiode, p_2, monitors the intensity of the source beam during the LITA interaction.

The detection system consists of a fast photomultiplier tube (PMT, Hammamatsu model OPTO-8) with at least a 500 MHz signal bandwidth and optical filters to prevent contamination of the signal by otherwise scattered light, luminosity, room light, etc. The filters include a 10 nm bandpass interference filter centered at 488 nm and a 40 mm lens/20 μm pinhole spatial filter. The LITA signal path-length to the detector is about 2.5 m. The PMT power supply (Fluke 412B) was carefully filtered to eliminate RF noise-sources.

Data are recorded using a 1 GS/s, eight-bit, two-channel digital storage oscilloscope (DSO) (HP 54510A). This records typically 500-to-2000-sample time histories of signals from the PMT and p_2, triggered by the signal from p_1. When needed, ensemble averaging eliminates shot noise from weak LITA signals. Otherwise, measurements require only a single driver laser pulse. Data from the DSO is down-loaded via a GPIB interface to a computer for analysis.

During the earliest experiments, LITA signals were measured from the laboratory air, which had essentially the same composition as the outside air. According to the Southern California Air Quality Management District, this contained less than 50 parts-per-billion of the pollutant NO_2 during the days of experimentation. In spite of the low concentration and the relative weakness of NO_2 transitions near 589 nm, LITA successfully detected the trace species. In later experiments, NO_2 was seeded into the air near the sample volume by reacting copper and concentrated nitric acid in a beaker. Future tests are planned to explore the parameters of LITA quantitatively in a high-pressure, heated bomb with optical access.

Experimental Results and Discussion

The earliest set of LITA experiments using laboratory air was completely nonresonant, the signal arising completely from nonresonant electrostriction. In these experiments, the signal scattered from the Ar ion laser was very weak, roughly 30 photons per nanosecond (reflectivity of $\sim 10^{-8}$ with the 1 W source beam). Ensemble averaging provided usable signals. An average of 256 shots yields the nonresonant data plotted as the dotted curve in Figure 3. The frequency of the modulation is about 26 MHz, twice the Brillouin frequency, yielding a sound speed accurate within the uncertainty of the knowledge of the laboratory sound speed ($\sim 0.5\%$). The signal recorded near a line of NO_2 appears as a dashed curve in Figure 3 for comparison. Resonant enhancement of the real part of the susceptibility of the gas is responsible for this signal increase. The signal recorded near the peak of the absorption line is the solid curve plotted in Figure 3. On this curve the dominant frequency modulation is at the Brillouin frequency, caused by interference between the signals scattered by the phonons and the thermon.
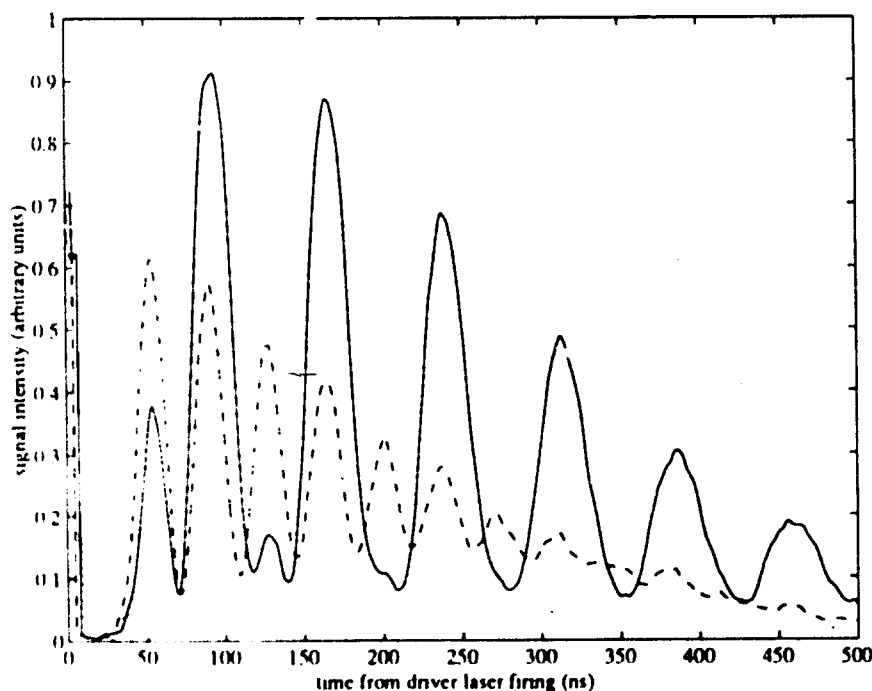

Figure 3.   The nonresonant electrostrictive signal (dotted curve), near-resonant electrostrictive signal (dashed curve) and resonant signal (solid curve) are plotted for comparison. The resonant signal modulation is mostly at the Brillouin frequency. Off-resonance signal modulation is mostly at twice this frequency.

A LITA "spectrum" of the susceptibility of the gas appears in Figure 4. The spectrum was taken by scanning the driver laser between test runs and is intended to suggest the capability of the technique. It is not to be interpreted quantitatively because the discrete frequency step in the spectrum was about 12 GHz, much too large to resolve lines of the gas. A spectrum of the complex susceptibility of the gas may be obtained by analyzing each measurement. Future spectral studies are planned when the laser-scanning, data-acquisition/down-loading/data-processing systems are automated.
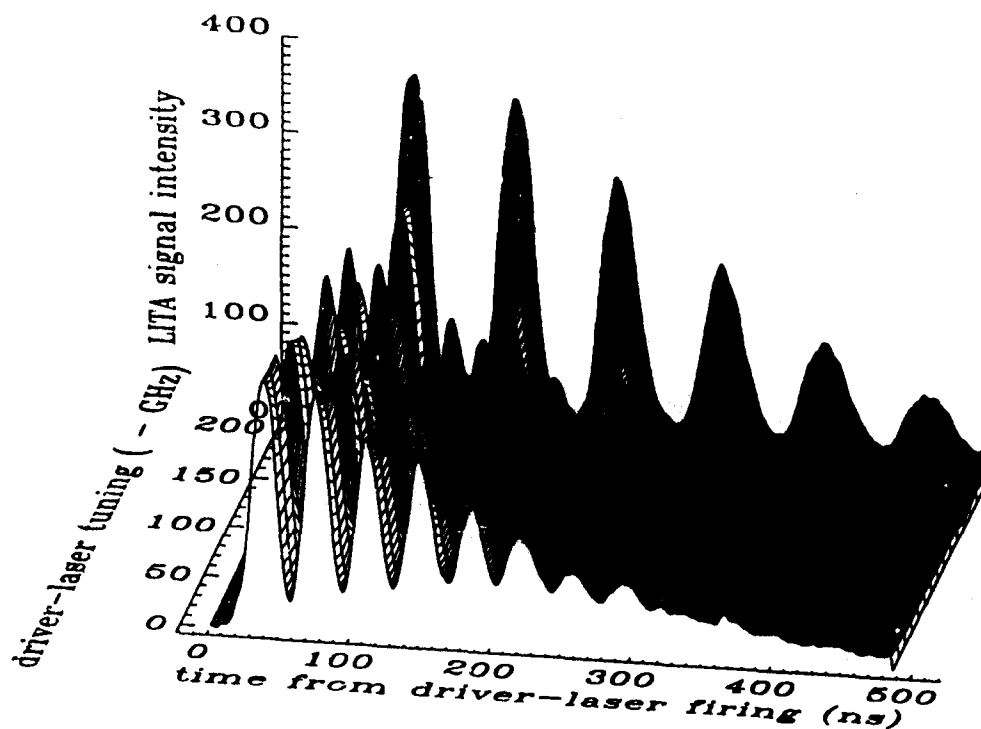
Figure 4.   This LITA "spectrum" of trace NO_2 consists of 256-shot ensemble averages of LITA signals taken approxi-
mately 12 GHz apart. In the foreground the signal comes primarily from resonantly-enhanced electrostriction;
in the background, the signal is characteristic of resonance (thermalization). The structure in between consists
of unresolved lines because of the large frequency step.

Seeding the gas with NO_2 provided LITA signals that were several orders of magnitude stronger than the signals obtained from
room air, with estimated reflectivities around 10^{-4}. True single-shot measurements of the sound speed and transport properties
were taken. A sample single-shot LITA signal appears in Figure 5. The driver beam crossing angle was $1.04°$, yielding a grating
wavelength of 32.3 μm and a Brillouin frequency of 10.7 MHz. At high concentration of absorbing species, the thermalization
effect swamps the electrostrictive effect. Figure 6 shows a four-shot average of the LITA signal obtained when the beam crossing
angle was widened to 2.3 ° (grating wavelength of, 14.5 μm; Brillouin frequency of 23.9 MHz) Damping of the waves occurs on
a time-scale proportional to the square of the grating wavelength. In Figure 6 the theoretical LITA signal is plotted with a dashed
curve, showing excellent agreement with experiment. The sound speed and transport coefficients used in the fit are published values
for dry air. In these tests, thermalization occurs on a time scale comparable to the inverse of the Brillouin frequency. Thus, the
simple single-rate model of thermalization which applies when such rates are poorly resolved is replaced by a model consisting of the
superposition of two single-rate thermalizations: a fast $\sim$10 ns process and a slow $\sim$100 ns process. The two rates and the relative
balance between the processes are three independent fitting parameters. A better fit to the data could be obtained by adopting a more
accurate thermalization model and source-beam-profile model (a top-hat profile is assumed) and including the effect of source-beam
phase noise. Future experiments will seek to refine these models. Because of the resolved unknown thermalization behavior, the
uncertainty of transport property measurements is high. Experiments conducted at high pressures, where thermalization rates are
much faster, are planned to confirm the accuracy of the expression for the LITA signal with no degrees of freedom (in the limit of
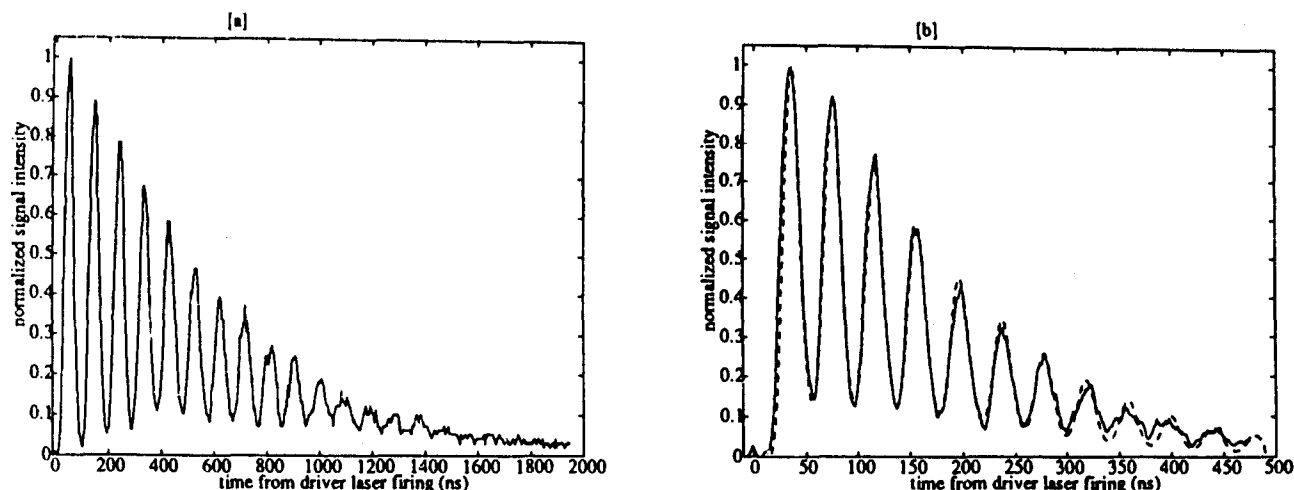rapid thermalization rate).

Figure 5. [a] This single-shot LITA signal of NO_2-seeded air was taken with a grating wavelength of 32.3 μm. [b] This four-shot average LITA signal of seeded air was taken with a grating wavelength of 14.5 μm. Damping-rates increase as the inverse square of the grating wavelength. The theoretical fit to this data is plotted as the dashed curve, showing excellent agreement.

Future Directions

It is premature to gauge at this early stage in the development of this technique what its future capabilities or applications might include. However, there are several interesting applications already under consideration. The measurement of transport properties of gases is very important in several fields including gas-phase chemical modeling and hypersonics. To the author's knowledge, LITA provides the most direct nonintrusive measurement of these properties. The measurement of sound speed provides the temperature if the gas composition or caloric equation of state is known. While this is not a direct temperature measurement, the considerable ease with which the measurement is performed has merit. Furthermore, the "direct" measurement of temperature via fitting populations to Boltzmann distributions often requires a great deal of spectroscopic and energy-transfer knowledge. LITA's ability to measure temperatures accurately from the very first signals without any calibration speaks in it's favor.

While the measurement of these gas-dynamic parameters has been discussed throughout this paper, there are several other applications that are evident. LITA has provided information about the rates of thermalization of excited-state energy. LITA could in the future become another window in the study of molecular and atomic energy transfer. The ability to detect and measure the complex susceptibility of trace species suggests that LITA could be employed in atmospheric pollution detection and spectroscopic studies.

Another application of LITA is flow-velocity measurement. When the acoustic structures generated using LITA convect in a flow, the light scattered off them generally has a Doppler shift. This Doppler shift may be measured by time-resolving the LITA signal heterodyned with the unscattered source laser. The strength of the scattered signal in LITA makes this technique practical. Preparations for future experiments in LITA velocimetry have begun. Yet another potential application of LITA is the measurement of strong vorticity. The phase-matched scattering angle of a LITA structure immersed in a fluid with local rotation will similarly rotate. Thus the direction of emergence of the LITA signal could be used to infer vorticity.

In all likelihood, the pursuit of these various applications will point toward others. In the near term, however, the analysis of LITA signals and techniques of LITA measurement will be refined. Careful parametric studies will be performed to validate the analysis and find the limits of the technique.

Conclusions

Laser-induced thermal acoustics (LITA) is a time-resolved four-wave mixing (FWM) technique for gas-phase measurement of sound speed and transport properties. It is different from conventional four-wave mixing techniques in that the optical nonlinearity is a sequence of opto-acoustic and acousto-optic effects. The interaction lifetime is dictated by the damping processes of acoustic attenuation and heat transfer, which occur generally on much longer time scales than dephasing and quenching. Thus the LITA signal may be resolved in time in a single shot using a fast detector and fast sampling oscilloscope, not the multiple-shot optical delay scanning techniques often required for time-resolved FWM. LITA has demonstrated excellent sensitivity in the first round of experiments. Detection limits of weak spectral lines of NO_2 in atmospheric air of less than 50 ppb were observed using relatively weak lasers. LITA sound-speed measurements were accurate within the uncertainty of the calculated laboratory sound speed (0.5%). LITA can also measure the complex susceptibility of a gas. Frequency scanning experiments enable the measurement of susceptibility spectra. In gas seeded with NO_2, reflectivities of the order 10^{-4} were estimated. In both magnitude and time-history, the LITA signal is accurately represented by an analytical expression for the LITA signal derived from the linearized equations of hydrodynamics and light scattering.

Acknowledgements

References

1. K.A. Nelson, M.D. Fayer, 1980 "Laser-induced phonons: A probe of intermolecular interaction in molecular solids, "*J. Chem. Phys.* 72, 5202-5218.

2. R. J. D. Miller, R Casalegno, K. A. Nelson and M. D. Fayer, 1982 "Laser-Induced Ultrasonics: A dynamic hologram approach to the measurement of weak absorptions, optoelastic constants and acoustic attenuation" *Chem. Physics* 72, 371-379.

3. E.B. Cummings, 1992 "Techniques of single-shot thermometry by degenerate four- wave mixing," GALCIT report FM 92-2, California Institute of Technology, Pasadena, CA.

4. R.W. Boyd, 1992 *Nonlinear Optics*, Academic Press, New York, NY.

5. A.C. Eckbreth, 1988 *Laser Diagnostics for Combustion Species and Temperature*, Abacus Press, Cambridge, MA.

6. H.W. Liepmann, A. Roshko, 1957 *Elements of Gasdynamics*, John Wiley and Sons, New York, NY.

7. B.J. Berne, R. Pecora, 1976 *Dynamic Light Scattering*, John Wiley and Sons, New York, NY.

8. L. D. Landau, E. M. Liftshitz, 1960 *Electrodynamics of Continuous Media*, Addison-Wesley Publishing Company, Inc., Cambridge, MA.